Am J Cancer Res 2021;11(9):4347-4363
www.ajcr.us /ISSN:2156-6976/ajcr0127932

Original Article

Effect of *APOBEC3A* functional polymorphism on renal cell carcinoma is influenced by tumor necrosis factor-α and transcriptional repressor ETS1

Xiaojie Tan[1#], Shaoling Zheng[2#], Wenbin Liu[1#], Yan Liu[1], Zhengchun Kang[3], Zishuai Li[1], Peng Li[1], Jiahui Song[1], Jianguo Hou[4], Bo Yang[4], Xue Han[5], Fubo Wang[4*], Chunxia Jing[2*], Guangwen Cao[1*]

[1]Department of Epidemiology, Second Military Medical University, Shanghai 200433, China; [2]Department of Epidemiology, School of Medicine, Jinan University, Guangzhou 510632, China; [3]Department of General Surgery, The 1st Affiliated Hospital, Second Military Medical University, Shanghai 200433, China; [4]Department of Urology, The 1st Affiliated Hospital, Second Military Medical University, Shanghai 200433, China; [5]Department of Chronic Diseases, The Center for Disease Control and Prevention of Yangpu District, Shanghai 200090, China. [*]Co-senior authors. [#]Equal contributors.

Received December 9, 2020; Accepted August 13, 2021; Epub September 15, 2021; Published September 30, 2021

Abstract: Human apolipoprotein B mRNA editing enzyme, catalytic polypeptide (APOBEC) 3 cytidine deaminases are the prominent drivers of somatic mutations in cancers. However, the effect of *APOBEC3*s functional polymorphisms on the development of renal cell carcinoma (RCC) remains unknown. Five genetic polymorphisms affecting the expression of APOBEC3A (A3A), APOBEC3B, and APOBEC4 and uracil DNA glycosylase (UNG) were genotyped in 728 RCC patients and 1500 healthy controls. The effects of tumor necrosis factor-α (TNFα) and interleukin-6 on the activity of the *A3A* promoter with rs12157810-A or -C in four RCC cell lines (786-O, A498, Caki2, ACHN) and two colorectal cancer cell lines (HCT116, SW620) were evaluated using dual-luciferase assays. Transcriptional repressors to the *A3A* promoter were identified by chromatin immunoprecipitation-quantitative PCR. The proapoptotic effect of *A3A* on RCC cells was evaluated using cytometry. The prognostic values of A3A and ETS1 were evaluated by the Cox regression analysis. The expressions of A3A and ETS1 were evaluated in clear cell RCC (ccRCC) specimens with different polymorphic genotypes using quantitative RT-PCR and immunohistochemistry. Of those functional polymorphisms, CC genotype at rs12157810 in the *A3A* promoter was significantly associated with a decreased risk of ccRCC, compared to the AA genotype (odds ratio adjusted for age and gender, 0.41, 95% confidence interval [CI], 0.28-0.57). Other polymorphic genotypes were not associated with the risk of RCC. The activity of the *A3A* promoter with rs12157810-C was significantly higher than that with rs12157810-A in the four RCC cell lines and two colorectal cancer cell lines. The activity of the *A3A* promoter with rs12157810-C was greatly up-regulated by TNFα and predominantly inhibited by a transcriptional repressor ETS1. The binding of ETS1 to the *A3A* promoter with rs12157810-C was looser than that with rs12157810-A. Ectopic expression of *A3A* significantly promoted apoptosis in ccRCC cells, rather than in colorectal cancer cells. Higher ETS1 expression predicted a favorable prognosis in ccRCC, with a hazard ratio of 0.58 (95% CI, 0.43-0.78). Rs121567810-C up-regulates the *A3A* promoter activity, possibly due to higher response to TNFα and looser transcriptional repression by ETS1. Up-regulation of A3A increases apoptosis, thus decreasing ccRCC risk in those carrying rs121567810-C.

Keywords: APOBEC3A, RCC, genetic polymorphisms, ETS1, inflammation, tumor suppressor

Introduction

Worldwide, the incidence of kidney cancer has steadily increased, with 403,262 new cases and 175,098 deaths in 2018, which is more common in men than in women [1]. Renal cell carcinoma (RCC) accounts for approximately 90% of kidney cancers. The histologic types of RCC are clear cell (ccRCC, 70%), papillary (10-15%), and chromophobe (5%) carcinoma [2]. The high incidence rates are reported in Europe and North America. Moreover, the incidence and mortality of RCC showed an obvious rising trend in China in the past decade, possibly because of increased exposure to the risk factors including smoking, obesity, hyper-

tension, and urolithiasis [3, 4]. The environmental factors usually influence RCC risk and progression by interacting with genetic predisposition [4, 5].

Mutation signatures in cancer genomes, often identified by deep sequencing, are the key genetic characteristics of cancer. Some nonrandom, cancer-specific mutation signatures might be caused by the human apolipoprotein B mRNA editing enzyme, catalytic polypeptide (APOBEC) 3 cytidine deaminase family [6-9]. In RCC, APOBEC3-related C-to-T transition is the most major mutation type, accounting for approximately 30% of the total somatic mutations in Chinese ccRCC patients [10]. APOBEC3A (A3A) and APOBEC3B (A3B) are localized in the nucleus and often damage the cellular genome during DNA replication [11-13]. High-level A3B expression is positively associated with C-to-T transition-based mutation signatures in some malignancies including bladder cancer, cervical cancer, hepatocellular carcinoma (HCC), lung cancer, head and neck cancer, and breast cancer as well as in human cancer cell lines [13-15]. APOBEC-related somatic mutational signatures in cancer genome are often associated with poor prognosis [16, 17]. However, A3A expression is significantly higher in oral squamous cell carcinoma carrying the APOBEC3B-deletion allele, which is associated with a better prognosis [18]. A3B-expressing cells can be selectively killed by inhibiting uracil DNA-glycosylase (UNG) because UNG-initiated base excision repair is a major mechanism counteracting genomic mutagenesis by A3B [19]. Our previous work has shown that polymorphic genotypes predisposing to the APOBEC3B-UNG imbalance in the inflammatory microenvironment promote the development of HCC [20, 21]. APOBEC4 (A4) is a new member of the AID/APOBEC family [16, 22]. The roles of APOBEC family members and UNG on the development of RCC remain unknown.

This study was designed to investigate the functional polymorphisms predisposing the role of APOBEC-UNG balance on the development of RCC and its underlying mechanisms. A case-control study was firstly carried out to evaluate the association of functional single nucleotide polymorphisms (SNPs) of *A3A, A3B, A4,* and *UNG* and the risk of RCC. Then, the regulatory effects of the major inflammatory factors of nuclear factor-kappa B (NF-κB) and signal transducer and activator of transcription 3 (STAT3) signaling pathways as well as transcriptional repressors on the function of the polymorphisms affecting APOBEC-UNG balance were systemically evaluated in RCC cell lines. This study may provide important clues to elucidate the mechanisms by which the imbalance of APOBEC-UNG facilitates the development of RCC. The outcomes of this study may be predictive and prognostic for RCC.

Materials and methods

Study population

A total of 728 histologically confirmed RCC cases and 1500 healthy controls were enrolled in this case-control study. The basic characteristics of the participants are shown in **Table 1**. RCC patients were enrolled from the 1st affiliated hospital of Second Military Medical University during 2007 and 2018. Healthy individuals were recruited from the health examination center of the 1st affiliated hospital and the surrounding communities in Yangpu District, Shanghai, from 2009 to 2015. Peripheral blood samples were collected from each participant, frozen, and delivered to our laboratory for DNA extraction and genotyping. This study was approved by the institutional review board of Second Military Medical University and was in accordance with the Declaration of Helsinki and relevant guidelines. A written informed consent was obtained from each patient.

SNPs selection and genotyping

Firstly, we searched for the SNPs within the region 2 kb upstream of the transcription start site to 3' transcription stop sites of *APOBEC3A* (*A3A*), *A3B*, *A4*, and *UNG* with R^2 threshold of 0.8 in the Chinese Han population (1000 Genomes Project, http://www.1000genomes.org). Five potentially functional and tagged SNPs were selected because they had the minor allele frequencies (MAF) of more than 15% in Chinese Han population: rs12157810 (A3A, promoter region, A>C, MAF: 28.2%), rs12628403 (A3A, intron region, A>C, MAF: 29.1%), rs2267401 (A3B, promoter region, T>G, MAF in the population without A3B-deletion: 35.4%), rs1174657 (A4, intron region, T>C, MAF: 18.0%), rs3890995 (UNG, promoter region, T>C, MAF: 33.5%). rs12157810 and

Table 1. Associations of *APOBECs* and *UNG* polymorphisms with the risk of RCC

Variable		Clear cell RCC (ccRCC), n (%)	Other subtypes of RCC, n (%)	Healthy control, n (%)	ccRCC vs healthy control AOR (95% CI)	Other subtypes of RCC vs healthy control AOR (95% CI)
Age (year)		56.77±0.47	54.98±1.49	56.03±0.39	1.004 (0.99-1.01)	0.99 (0.98-1.01)
Gender						
Female		190 (29.37)	25 (30.86)	425 (28.33)	1.00	1.00
Male		457 (70.63)	56 (69.14)	1075 (71.67)	0.62 (0.77-1.16)	0.89 (0.55-1.45)
rs12157810 (*APOBEC3A* -525 bp A>C)	AA	388 (60.63)	43 (54.43)	791 (55.12)	1.00	1.00
	AC	211 (32.97)	30 (37.97)	435 (30.31)	0.98 (0.80-1.21)	1.26 (0.77-2.03)
	CC	41 (6.41)	6 (7.59)	209 (14.57)	0.41 (0.28-0.57)	0.51 (0.19-1.12)
	AC+CC	252 (39.38)	36 (45.56)	644 (44.88)	0.79 (0.66-0.96)	1.02 (0.64-1.60)
	A allele	987 (77.11)	116 (73.42)	2017 (70.28)	1.00	1.00
	C allele	293 (22.89)	42 (26.58)	853 (29.72)	0.70 (0.60-0.81)	0.84 (0.58-1.20)
rs12628403 (*APOBEC3A* 4340 bp A>C)	AA	267 (42.05)	41 (51.25)	617 (41.69)	1.00	1.00
	AC	277 (43.62)	29 (36.25)	702 (47.43)	0.91 (0.74-1.11)	0.62 (0.37-1.01)
	CC	91 (14.33)	10 (12.50)	161 (10.88)	1.29 (0.95-1.73)	0.97 (0.45-1.92)
	AC+CC	368 (57.95)	39 (48.75)	863 (58.31)	0.98 (0.81-1.19)	0.68 (0.43-1.07)
	A allele	811 (63.86)	111 (69.38)	1936 (65.41)	1.00	1.00
	C allele	459 (36.14)	49 (30.62)	1024 (34.59)	1.07 (0.93-1.22)	0.83 (0.59-1.17)
rs2267401* (*APOBEC3B* -338 bp T>G)	TT	102 (38.20)	21 (52.50)	229 (38.17)	1.00	1.00
	TG	114 (42.70)	12 (30.00)	267 (44.50)	0.95 (0.69-1.32)	0.48 (0.22-0.99)
	GG	51 (19.10)	7 (17.50)	104 (17.33)	1.11 (0.73-1.66)	0.74 (0.28-1.73)
	TG+GG	165 (61.80)	19 (47.50)	371 (61.83)	0.99 (0.74-1.34)	0.55 (0.28-1.04)
	T allele	318 (59.55)	54 (67.50)	725 (60.42)	1.00	1.00
	G allele	216 (40.45)	26 (32.50)	475 (39.58)	1.02 (0.83-1.26)	0.72 (0.43-1.15)
rs1174657 (*APOBEC4* 5526 bp T>C)	TT	403 (62.58)	53 (65.43)	892 (64.87)	1.00	1.00
	TC	219 (34.01)	24 (29.63)	411 (29.89)	1.18 (0.96-1.44)	0.98 (0.58-1.60)
	CC	22 (3.42)	4 (4.94)	72 (5.24)	0.68 (0.41-1.09)	0.92 (0.27-2.35)
	TC+CC	241 (37.42)	28 (34.57)	483 (35.13)	1.11 (0.91-1.34)	0.97 (0.60-1.55)
	T allele	1025 (79.58)	130 (80.25)	2195 (79.82)	1.00	1.00
	C allele	263 (20.42)	32 (19.75)	555 (20.18)	1.01 (0.86-1.19)	0.84 (0.50-1.34)
rs3890995 (*UNG* -1956 bp T>C)	TT	263 (42.08)	26 (33.33)	634 (43.22)	1.00	1.00
	TC	282 (45.12)	39 (50.00)	655 (44.65)	1.04 (0.85-1.27)	1.44 (0.87-2.42)
	CC	80 (12.80)	13 (16.67)	178 (12.13)	1.07 (0.79-1.45)	1.80 (0.87-3.52)
	TC+CC	362 (57.92)	52 (66.67)	833 (56.78)	1.04 (0.86-1.26)	1.51 (0.94-2.49)
	T allele	808 (64.64)	91 (58.33)	1923 (65.54)	1.00	1.00
	C allele	442 (35.36)	65 (41.67)	1011 (34.46)	1.03 (0.90-1.19)	1.35 (0.97-1.87)

SNP, single-nucleotide polymorphism; CI, confidence interval; RCC, renal cell carcinoma; AOR, odds ratio adjusted for age and gender. *Calculated in subjects with rs12628403-AA genotype (without APOBEC3B-deletion).

rs2267401 represented the haplotype block in the promoter region of A3A and A3B, as determined using Haploview 4.2 software. rs12628403 was selected as the proxy of A3B-deletion. Since the promoter region of A3B is two-copy deletion in the subjects with rs12628403-CC genotype, rs2267401 was only genotyped in subjects carrying the rs12628403-A allele. Fluorescent-probe real-time quantitative PCR was conducted for SNP genotyping in each 96-well PCR plate by using Roche LightCycler 480 System (Roche Diagnostics, Basel, Switzerland) [20]. The TaqMan probes and primers were designed and synthesized by Sangon Biotech (Shanghai, China). The sequence of primers and probes of the SNPs are listed in Table S1.

Cells and plasmids

ACHN (CRL-1611), 786-O (CRL-1932), Caki2 (HTB-47), A498 (HTB-44) cells were purchased from American Type Culture Collection (ATCC, Manassas, VA). HCT116 and SW620 cells were purchased from the Cell Bank of the Chinese Academy of Sciences (Shanghai, China). ACHN, 786-O, Caki2, HCT116, A498 and SW620 cells were cultured in MEM, RPMI 1640, McCoy's 5A, EMEM and Leibovitz's L-15 (GIBCO, Grand Island, NY), respectively. The media were supplemented with 10% fetal bovine serum and 1% penicillin/streptomycin. Cell cultures were performed in the humidified 5% CO_2 environment at 37°C.

The *A3A* promoter fragments (-1000 bp to -1 bp) carrying rs12157810-A or rs12157810-C were synthesized by Obio Technology (Shanghai, China) and constructed into a pGL4.10-basic vector (Promega, Madison, WI) to construct the recombinant plasmids with a luciferase reporter gene under the transcriptional control of the *A3A* promoter (Figure S1). The A3A expressing vector containing human A3A coding sequence in the pcDNA3.1 expression vector was purchased from Promega (Madison, WI). The small interfering RNAs (siRNAs) targeting *ETS1*, *RFX5*, *ZEB1*, and *MSX2* (Table S1) were synthesized by Ribobio (Guangzhou, China). Transient transfection was performed using LTX Plus (Invitrogen, Carlsbad, CA) according to the manufacturer's instructions.

Dual-luciferase reporter assay

All the cancer cell lines were transfected with the firefly luciferase reporter plasmids and renilla luciferase control reporter vector (Promega) to evaluate the promoter activity. Twenty-four hours after the transfection, the luciferase activity was detected by dual-luciferase assay reagent (Promega) using microplate reader biotek synergy 2 (Biotek Instruments, Winooski, VT).

Chromatin immunoprecipitation (ChIP) assay

ChIP experiments were carried out using SimpleChIP (R) plus kit (magnetic bead) (Cell Signaling Technology) according to the manufacturer's manual. Chromatin-protein complexes were immunoprecipitated using ETS1 antibody (14069S, Cell Signaling Technology). IgG served as an experimental negative control (diluted 1:500, 2729, Cell Signaling Technology). Chip signal (% input) was calculated using the formula: % input = 2%*2^($CT^{2\%input}$-CT^{sample}). CT value was the average value of 3 repeats. ChIP-quantitative PCR (ChIP-qPCR) was conducted using the cellular genomic DNA bound with ETS1. Primers for ChIP-qPCR were designed to amply the *APOBEC3A* promoter covering rs12157810 (Table S1). The fold of enrichment in site occupancy was calculated as the DNA values of the ETS1 group divided by that of the IgG control group.

Quantification of gene transcription

Total RNAs of the cell lines were isolated using Trizol reagent (Invitrogen, Carlsbad, MA). Total RNAs of formalin-fixed paraffin-embedded (FFPE) specimens were isolated using RNeasy FFPE kit (73504, Qiagen, Stockach, Germany). Reverse transcription of mRNA into cDNA was carried out using the PrimeScript RT Master Mix Kit (Takara, Dalian, China). The transcriptional level was measured by reverse transcription quantitative PCR (RT-qPCR) with SYBR Premix Ex Taq II (Takara) on Roche LightCycler 480 System (Roche, Basilea, Switzerland). The levels of mRNA were normalized to the expression of GAPDH. The primers used in this study are summarized in Table S1.

Western blot

Whole cell protein lysates were extracted, quantified and subjected to Western blot according to the protocol as previously described [23]. Anti-APOBEC3A (dilution 1:500, PA5-78800, Invitrogen), anti-ETS1 (dilution 1:1000, 14069S, Cell Signaling Technology, Boston, MA) and anti-GAPDH (dilution 1:1000,

sc-25778, Santa Cruz, Dallas, TX) rabbit polyclonal antibodies were applied as primary antibodies. The signals were developed using prime Western blot detection reagents (Amersham Biosciences, Piscataway, NJ) according to the manufacturer's instructions. The signal intensity was obtained by scanning the bands using Image J software 1.8.0_172. Relative expression was calculated as the signal intensity of A3A or ETS1 divided by the signal intensity of basic GAPDH in each lane. Then, the change fold was subsequently obtained as the relative expression of A3A or ETS1 divided by the corresponding GAPDH expression for each cell line. The results were confirmed by at least three independent experiments.

Apoptosis assay

All the RCC cell lines were transfected with the A3A-expressing constructs or empty vector, respectively. Twenty-four hours after the transfection, cells were washed with cold PBS and harvested by 0.25% trypsin without EDTA (Gibco, Grand Island, NY). The cells were then resuspended in the binding buffer (BD Pharmingen, San Diego, CA), stained with Annexin V-FITC and 7-AAD (BD Pharmingen) according to the manufacturer's instructions. Cell apoptosis was measured by flow cytometry using Beckman Coulter CytoFIEX S (Beckman Coulter, Miami, FL).

Survival analysis using TCGA database

RNA-seq data and relevant clinical outcomes of ccRCC patients were downloaded from TCGA database (http://starbase.sysu.edu.cn/panCancer.php). Expression data were standardized by fragments per kilobase million. Overall survival was termed as a terminal event. The cut-off values of APOBEC3A expression and ETS1 expression in the Cox regression models were optimized using X-tile software [24].

Immunohistochemistry (IHC)

The FFPE specimens of ccRCC and the paired adjacent renal tissues were processes for IHC staining as previously described [25]. Anti-ETS1 (sc-55581, Santa Cruz, CA) and Anti-A3A (orb31364, Biorbyt, St. Louis, MO) were applied to perform IHC staining. Staining evaluation was performed independently by three investigators (Tan XJ, Liu Y, and Wang FB) who were blinded to the genotypes at rs12157810 of the patients. Briefly, an immunoreactive score was ranked by negative (-), slightly positive (+), moderately positive (++) and strongly positive (+++) according to the extent and intensity of staining. A close agreement (90%) on immunoreactive scores was usually reached between two of the three investigators. Otherwise, consensus was obtained after discussion.

Statistical analysis

Continuous data were expressed as mean ± standard deviation (SD) from at least three independent experiments. Then Student's t-test or Analysis of Variance (ANOVA) was performed to estimate the difference between groups by SPSS 21.0 (SPSS, Chicago, IL). The Hardy-Weinberg equilibrium (HWE) was calculated in the control groups using the Chi-square test. Logistic regression model was performed to calculate the odds ratio (OR) and 95% confidence interval (CI) for risk estimation in a case-control study. For the prognosis analysis, the hazard ratio (HR) and 95% CI were calculated using the Cox proportional hazard model. The significant factors in the univariate Cox analysis were introduced into the multivariate Cox model to determine the factors independently contributing to overall survival (OS). The Kaplan-Meier method was applied to estimate OS of RCC patients, and the log-rank test was performed to compare the survival curves. The R software 3.6.3 was applied to perform Kaplan-Meier analysis. $P<0.05$ was considered statistically significant.

Results

Genotype distribution and their associations with RCC risk

The demographic characteristics and the genotype frequencies of SNPs of 2228 subjects are presented in **Table 1**. No significant differences in age or gender were observed between the case and control groups ($P>0.05$). The male-to-female ratio in the case group was 2.4:1. Of the 728 cases, 647 (88.87%) were ccRCC, 34 (4.67%) were papillary RCC, and 23 (3.16%) were chromophobe RCC. Of those, 643 (88.32%) were at the AJCC (American Joint Committee on Cancer) stage I/II. The

frequencies of rs12628403, rs2267401, and rs3890995 were conformed to HWE in healthy controls (P>0.05), whereas rs12157810 and rs1174657 were out of HWE (P<0.01 for each). The frequency of the rs12157810-C allele was significantly lower in RCC patients than in healthy controls (23.29% vs 29.72%, P<0.001). CC genotype at rs12157810 was significantly associated with a decreased risk of total RCC (age-, gender-adjusted OR [AOR], 0.41; 95% CI, 0.29-0.58), compared to AA genotype at rs12157810. The C allele at rs12157810 was significantly associated with a decreased risk of RCC, compared to the A allele (AOR, 0.71; 95% CI, 0.61-0.83). Compared to rs12157810-AA genotype, rs12157810-CC genotype was significantly associated with a decreased risk of RCC in each gender (P<0.01 for each) (Table S2). We did not observe any significant association of RCC risk with the genotypes at rs12628403, rs2267401, rs1174657, and rs3890995, respectively. The associations of the SNPs with the risk of RCC were solely replicated in patients with ccRCC (**Table 1**). TC genotype at rs3890995 was significantly associated with an increased risk of chromophobe carcinoma, compared to the TT genotype (AOR, 3.62; 95% CI, 1.30-12.78) (Table S3).

The effects of rs12157810 genotypes and inflammatory factors on the A3A promoter activity

The luciferase assay was applied to evaluate the effects of rs12157810 genotypes on the activity of the *A3A* promoter. The constructs were transiently transfected into ACHN, 786-O, Caki2, A498, HCT116, and SW620 cells, respectively. The activity of the *A3A* promoter was significantly higher in the six kinds of cell lines transfected with the construct containing the *A3A* promoter with rs12157810-C than in those with rs12157810-A (P<0.001, **Figure 1A**).

Tumor necrosis factor alpha (TNFα) and phorbol-12-myristate-13-acetate (PMA) are key activators of NF-κB signaling pathway while interleukin-6 (IL-6) activates STAT3 signaling pathway, both of which contribute to the development of RCC [26-29]. Therefore, we investigated if these inflammatory factors affected the expression of A3A. It was found that the transcription of *A3A* was significantly increased by TNFα treatment in all the cell lines used in our assay (**Figure 1B**). Upon the stimulation with TNFα, the expression of A3A protein at the same time-point as harvesting RNA was up-regulated in RCC cell lines (ACHN with AA genotype at rs12157810, 786-O with AC genotype at rs12157810, and Caki2 and A498 with CC genotype at rs12157810), rather than in SW620 and HCT116 with AA genotype at rs12157810 (**Figure 1C**).

After the transfection and then stimulation with the inflammatory factors, the dual-luciferase reporter assays indicated that the activity of the *A3A* promoter in 786-O, A498, and ACHN cells was significantly up-regulated by PMA (P<0.05). Interestingly, the activity of the *A3A* promoter carrying rs12157810-C, other than rs12157810-A, was significantly up-regulated by TNFα in all the RCC cell lines (P<0.05). Interestingly, this effect could not be observed in the colorectal cancer cell lines. IL-6 decreased the activity of the *A3A* promoter with C allele or A allele at rs12157810 in Caki2 cells (P<0.05). These data are presented in **Figure 2**.

Ectopic expression of A3A induced apoptosis in the ccRCC cells

A3A and A3B often lead to increased cancer-promoting APOBEC-signature mutagenesis. A3A can drive DNA replication stress and DNA damage, thus inducing fragmentation of cancer genome and apoptosis [30, 31]. We then evaluated the role of A3A in inducing apoptosis of RCC cells. Ectopic expression of *A3A* in the RCC cell lines was realized by transient transfection. The apoptotic rate of the cells was evaluated using flow cytometry. As shown in **Figure 3**, ectopic expression of A3A significantly increased late apoptosis (annexin V-FITC positive and 7-AAD positive) in 786-O and Caki2 cells (P<0.01) or early apoptosis (annexin V-FITC positive and 7-AAD negative) in A498 cells (P<0.01). However, this effect was not observed in ACHN cells (P>0.05).

Effect of ETS1 on the transcription of A3A

To know if exogenous *A3A* promoter with rs12157810-A and that with rs12157810-C binds differently with inherent nuclear *trans*-repressor for the inherent *A3A* promoter, we examined the mRNA level of *A3A* following the transfection with luciferase reporter under the

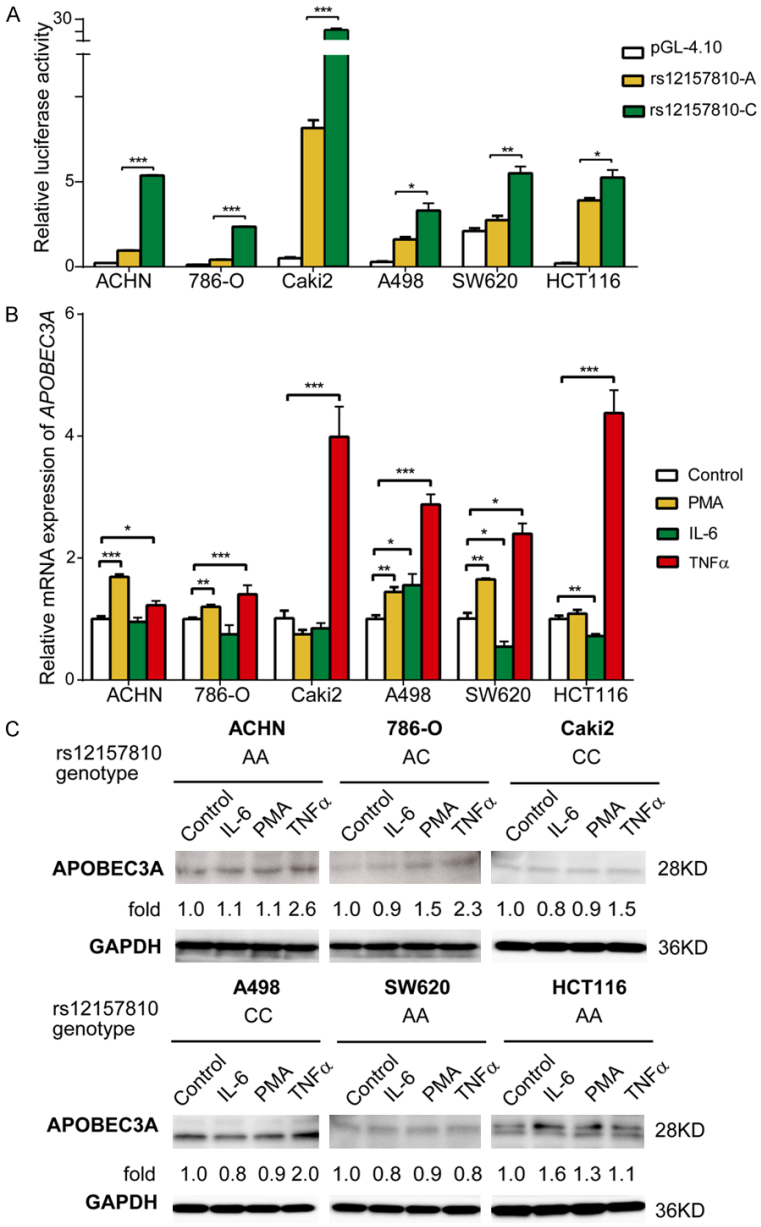

Figure 1. The effects of rs12157810 genotypes and inflammatory factors on the activity of the *A3A* promoter. A. The difference in the activity of the A3A promoter with rs12157810-A and that with rs12157810-C. B. The level of inherent A3A transcription in ACHN, 786-O, A498, Caki2, SW620, and HCT116 cells after the treatment of 100 ng/mL IL-6, 100 ng/mL PMA, and 20 ng/mL TNFα, respectively. C. The level of inherent A3A protein in ACHN, 786-O, A498, Caki2, SW620, and HCT116 cells after the treatment of 100 ng/mL IL-6, 100 ng/mL PMA, and 20 ng/mL TNFα, respectively. These assays were performed in three independent experiments. $^{*}P<0.05$, $^{**}P<0.01$, $^{***}P<0.001$.

transcriptional control of the *A3A* promoter carrying rs12157810-A and the counterpart carrying rs12157810-C. It was found that the exogenous *A3A* promoter with rs12157810-C increased the expression of inherent *A3A*, compared to that with rs12157810-A, in 786-O cells, rather than in ACHN cells. This result indicates that the exogenous *A3A* promoter with rs12157810-C selectively binds the *trans*-repressors, thus affecting the expression of inherent *A3A* (**Figure 4A**).

Transcriptional factors that could bind to the A3A promoter region covering -1 kb from the transcription start site were predicted using the online JASPAR database. Of those, regulatory factor X5 (RFX5), zinc finger E-box binding homeobox 1 (ZEB1), msh homeobox 2 (MSX2), and ETS proto-oncogene 1 (ETS1) were selected according to a higher predicted score (>0.8) and related scientific reports on cancer [32-34]. ETS1 could bind to the promoter region that covered rs12157810 site (-515 bp to -525 bp). Importantly, the predicted binding score of ETS1 was higher for the *A3A* promoter sequence with rs12157810-A than that with rs12157810-C, indicating a stronger binding power between ETS1 and the sequence with rs12157810-A (**Table 2**). EST1, RFX5, ZEB1, and MSX2 were then silenced using siRNA in 786-O and ACHN cell lines. The knockdown effects of these nuclear factors, as measured by qRT-PCR, are presented in Figure S2. Knockdown of *ETS1* significantly up-regulated the transcription of *A3A* in 786-O and ACHN cell lines. Knockdown of *RFX5, ZEB1*, and *MSX2* up-regulated the transcription of *A3A* in 786-O, respectively, rather than in ACHN cells (**Figure 4B**). Although the background expressions of ETS1 and A3A proteins were

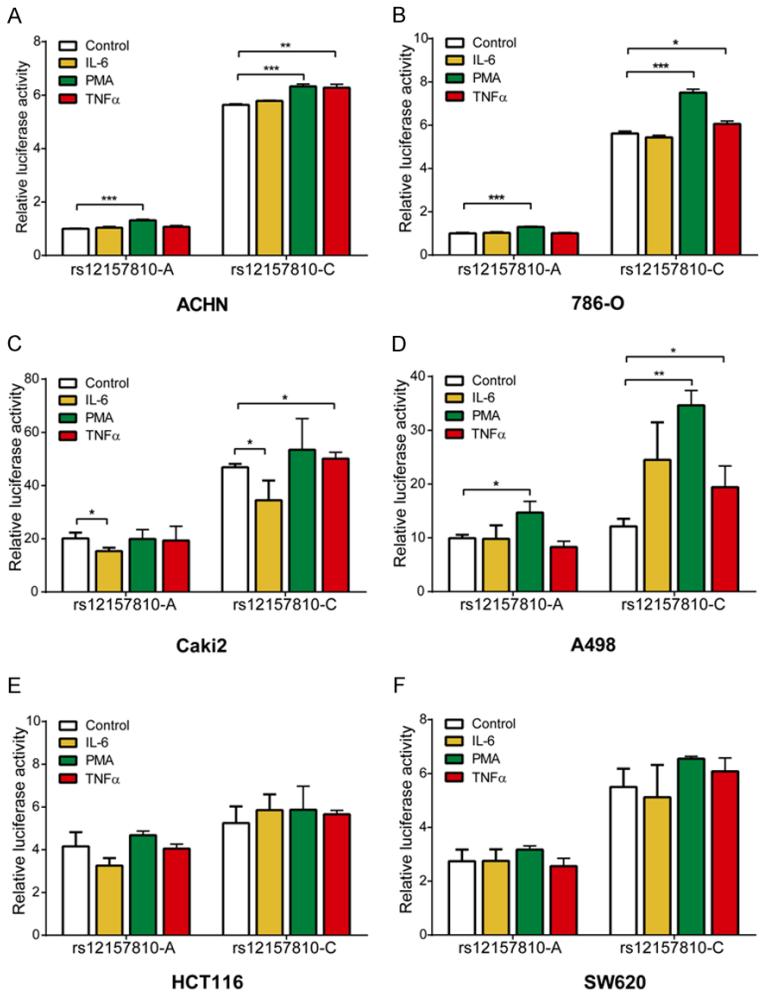

Figure 2. The effects of inflammatory factors on the activity of the *A3A* promoter with A or C at rs12157810. A. ACHN cells. B. 786-O cells. C. Caki2 cells. D. A498 cells. E. HCT116 cells. F. SW620 cells. These assays were performed in triplicate. $^{*}P<0.05$, $^{**}P<0.01$, $^{***}P<0.001$.

higher in ACHN than in 786-O cells, the expression of A3A protein was up-regulated after silencing ETS1 in ACHN and 786-O cells (**Figure 4C**). ChIP-qPCR assays were performed to check the physical binding effects of ETS1 with the A3A promoter region containing rs12157810 site in the four RCC cell lines. As shown in **Figure 4D**, the binding effects were confirmed in all the ccRCC cells. Compared to IgG group, the enrichment percentage of *ETS1* group was 10.94-fold higher in A498 cells, 7.33-fold higher in Caki2 cells, 7.01-fold higher in 786-O cells, and 2.19 in ACHN cells. The fragment of approximately 150 bp predicted binding region including rs12157810 site amplified by ChIP-qPCR was successfully sequenced using Sanger sequencing method (**Figure 4E**). As the RCC cell lines and the colorectal cancer cell lines responded differently to the inflammatory factors (**Figure 2**) and the C allele at rs12157810 could significantly increase the activity of the *A3A* promoter in all the cell lines (**Figure 1A**), we then tested the activity of the *A3A* promoter by co-transfection with siETS1 and the construct of dual-luciferase reporter containing A allele or C allele at rs12157810 in both RCC and colorectal cancer cell lines. We found two similar effects of siETS1 on the *A3A* promoter activity as follows: siETS1 greatly up-regulated the activity of the *A3A* promoter with rs12157810-C, rather than that with rs12157810-A, in three RCC cell lines (786-O, A498, and ACHN) and one (SW620) of two colorectal cancer cell lines ($P<0.05$); siETS1 greatly down-regulated the activity of the *A3A* promoter with rs12157810-A ($P<0.05$), rather than that with rs12157810-C, in Caki2 and HCT116 cells (**Figure 4F**).

Prognostic value of A3A and ETS1 expression on ccRCC

To further clarify the role of A3A and EST1 on the development of ccRCC, we evaluated the prognostic value of A3A and EST1 using the TCGA database. A total of 533 patients with ccRCC were included in this analysis. The cut-off values optimized using X-tile were applied to dichotomize the patients into groups of higher and lower values of A3A and EST1, respectively. The expression of A3A could not significantly predict the prognosis of ccRCC patients either in the univariate or multivariate Cox regression analysis. However, increasing age and neoadjuvant treatment independently predicted an unfavorable prognosis; whereas higher ETS1 expression in tumor tissues independently predicted a favorable prognosis in ccRCC in the multivariate Cox regression an-

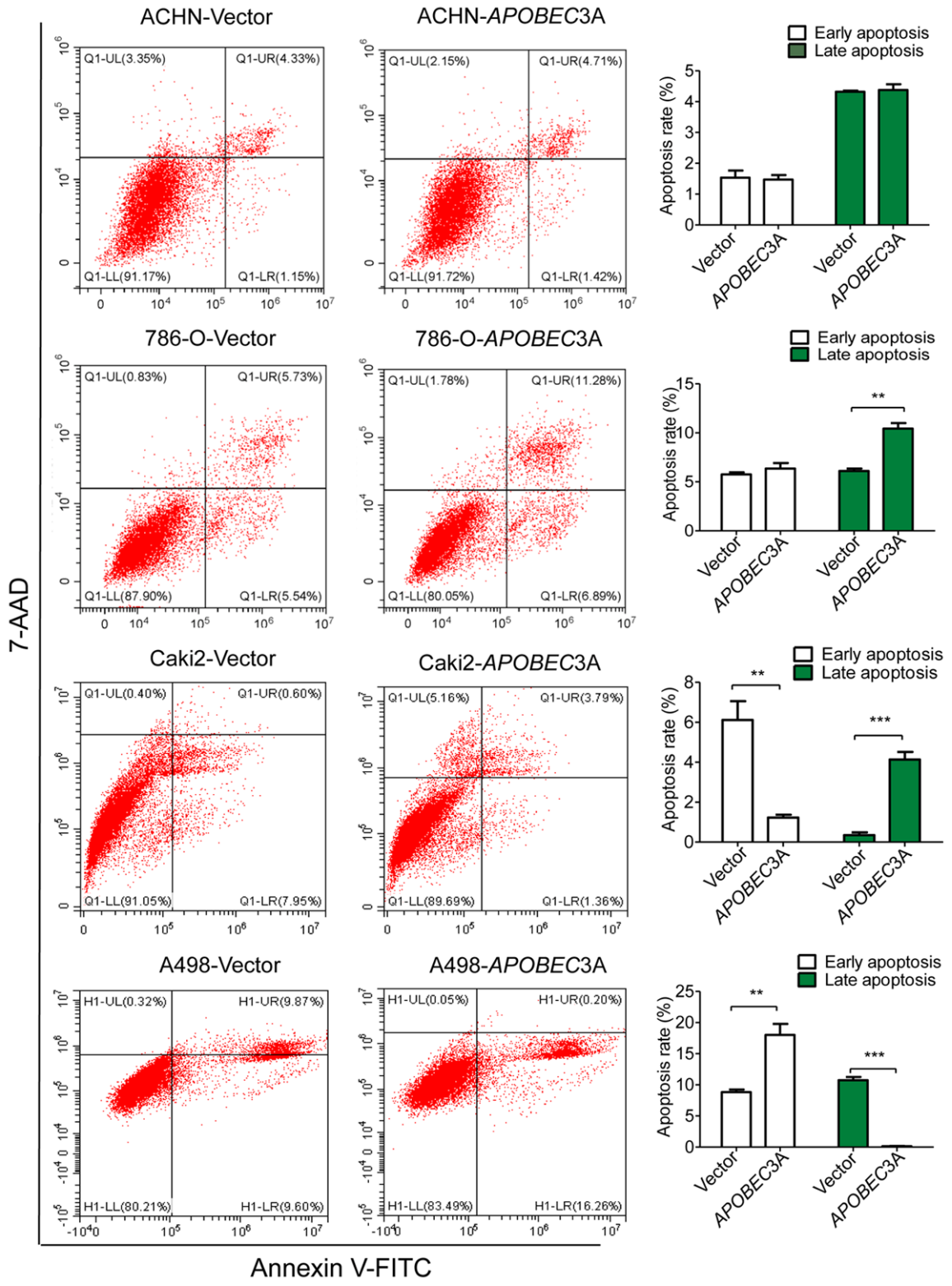

Figure 3. Ectopic expression of A3A affected the apoptotic rate of the four RCC cell lines. The rates of the early apoptosis (Annexin V+/7-AAD-) and late apoptosis (Annexin V+/7-AAD+) were summarized in histograms. The assay was determined by flow cytometry 24 h after the transfection and performed in triplicate. $^{*}P<0.05$, $^{**}P<0.01$, $^{***}P<0.001$.

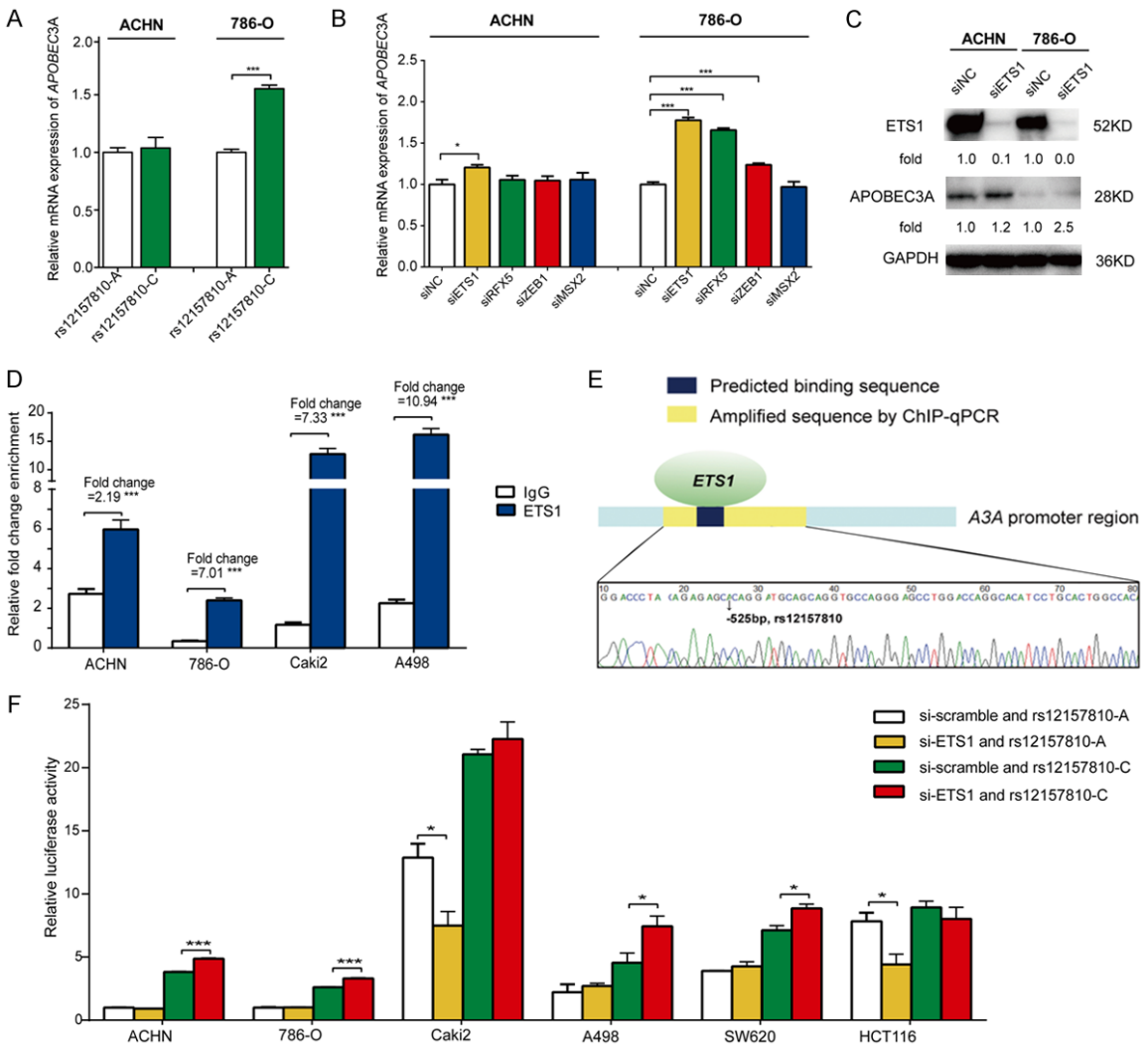

Figure 4. The effect of transcriptional repressor ETS1 on the activity of the *A3A* promoter with A or C at rs12157810. A. The expression of inherent *A3A* in ACHN and 786-O cells after the transfection with the A3A promoter carrying A or C at rs12157810. B. The effects of silencing transcription factors on the expression of A3A. C. The effect of siRNA targeting *ETS1* (siETS1) on the expression of A3A protein 36h after the transfection. D. ChIP-PCR assay: amplification of the A3A promoter with rs12157810-A or rs12157810-C binding to ETS1. IgG serves as a negative control. E. The sequence of the A3A promoter region containing the rs12157810 site, which was amplified by ChIP-qPCR. F. The effect of co-transfected siETS1 on the activity of the *A3A* promoter carrying A or C at rs12157810. The assays were performed in triplicate. $^{*}P<0.05$, $^{**}P<0.01$, $^{***}P<0.001$.

alysis (**Table 3**; **Figure 5**). Thus, ETS1, a transcriptional repressor that had a looser affinity to the *A3A* promoter with rs12157810-C, functioned as a tumor suppressor in ccRCC.

Association of rs12157810 genotypes with the expression of A3A/ETS1 in ccRCC

We assessed the association between EST1/A3A expression and rs12157810 polymorphic genotypes using the surgically removed samples of ccRCC patients who were involved in our case-control study. Of all the 47 patients with CC genotype at rs12157810, we selected 18 patients whose surgically removed tumor and adjacent renal tissues were sufficient and qualified for this analysis. Then, we randomly selected 50 patients from each of the other two groups. Of the 100 patients, 22 patients with the AA genotype and 26 patients with the AC genotype had sufficient and qualified tumor and adjacent tissues for this analysis. We

Table 2. Transcription factors binding sites predicted by the JASPAR database

ID	Name	Score	Relative score	Predicted binding sequence
MA0510.1	RFX5	14.49	0.94	CTCCCTGGCACCTGC
MA0510.1	RFX5	11.76	0.91	TGCACTGGCCACAGG
MA0103.3	ZEB1	12.23	0.96	GGCACCTGCTG
MA0103.2	ZEB1	7.09	0.87	CCTCCCCTG
MA0708.1	MSX2	9.75	0.93	ACAATTAT
MA0098.3	ETS1	9.73	0.90	ACAGGATGCA#
MA0098.3	ETS1	6.14	0.84	CCAGGATGCA#

RFX5, regulatory factor X5; ZEB1, zinc finger E-box binding homeobox 1; MSX2, msh homeobox 2; ETS1, ETS proto-oncogene 1. #The binding sequence containing rs12157810 site.

used qRT-PCR to evaluate the transcription of *A3A* and *ETS1* in the FFEP tumor specimens. It was found that the level of *A3A* transcription in the ccRCC FFEP tissues of patients with the CC genotype was significantly higher than that in those with the AC genotype and that in those with the AA genotype ($P<0.01$, **Figure 6A**). No significances were found among the levels of *ETS1* transcription in the tumor tissues of patients with the AA, in those with the AC, and in those with the CC genotype. The expression levels of A3A and ETS1 protein in the FFEP specimens of ccRCC and corresponding adjacent renal tissues were examined using semi-quantified IHC. The levels of A3A protein in the ccRCC tissues were quite consistent with its transcriptional level ($P<0.001$, **Figure 6B**). The level of ETS1 protein was also consistent with its transcriptional level ($P>0.05$). The protein level of ETS1 was significantly lower in the tumor tissues than in the adjacent renal tissues of patients with any rs12157810 genotype ($P<0.05$). The protein level of A3A was significantly lower in the tumor tissues than in the adjacent tissues of patients with the AA genotype ($P<0.001$) or the AC genotype ($P<0.01$) (**Figure 6C**).

Discussion

In this study, we investigated the effect of functional SNPs affecting the expression of *A3A* on the development of RCC. The epidemiological result was quite in contrast to our original speculation, that is, genetic predisposition facilitating the expression of APOBECs should increase the risk of RCC via inducing cancer-promoting somatic mutations. The genotype CC at the *A3A* promoter SNP rs12157810 caused a higher expression of *A3A* but it was significantly associated with a decreased risk of RCC. Ectopic expression of A3A in ccRCC cells 786-O, A498, and Caki2 with at least a C allele at rs12157810, rather than in papillary RCC cell line ACHN with rs12157810-AA, caused high-level early or late apoptosis (**Figure 3**). A3A, which has a low abundance in the most solid cancers and somehow high abundance in acute myelogenous leukemia, has >100-fold more cytidine deamination activity than A3B in the presence of cellular RNA and drives DNA replication stress and DNA damage [35, 36]. Thus, the genetic predisposition facilitating the expression of *A3A* contributes to increased fragmentation of cellular genome. This might happen at the earliest stage of individual development because rs12157810-C was much less frequent than rs12157810-A in healthy controls, thus contributing to the out-of-HWE. Interestingly, this difference in polymorphic genotype at rs12157810 was more significant in ccRCC patients than in healthy controls (**Table 1**). A previous study has shown that high-level APOBEC3A expression is associated with better overall survival, especially among oral cancer patients carrying A3B-deletion alleles [18]. In our study, no significant association was found between the expression of *A3A* and ccRCC prognosis in the Cox regression analysis (**Table 3**). Cancer cells with high-level somatic mutations caused by high-level A3A expression are more apt to be eradicated via inducing late apoptosis in patients carrying A3B-deletion alleles. These data imply that A3A-caused apoptosis in RCC cells might be counteracted by A3B-induced somatic mutation during disease progression. It has been suggested that recurrent low-level mutation by A3A could catalyze the transition from a healthy to a cancer genome [8]. Caner evolution might depend on a mild level of somatic mutations prominently caused by low-level A3A and high-level A3B expression in the inflammatory microenvironment.

The activity of the A3B promoter has been proven to be activated by IL-6/STAT3 signaling pathway and treatment with a DNA-damaging

Table 3. Cox regression analysis for the overall survival of patients with RCC

Characteristics	Univariate Cox regression analysis		Multivariate Cox regression analysis	
	Hazard ratios (95% CI)	*P*	Hazard ratios (95% CI)	*P*
Age (n = 533)	1.03 (1.02-1.04)	<0.001	1.03 (1.02-1.04)	<0.001
Gender				
Female (n = 188)	1.00		1.00	
Male (n = 345)	0.95 (0.69-1.29)	0.74	1.03 (0.75-1.40)	0.88
Neoadjuvant treatment				
No (n = 516)	1.00		1.00	
Yes (n = 17)	2.13 (1.12-4.03)	0.02	2.19 (1.15-4.19)	0.02
APOBEC3A (cut-off 3.94)				
≤40% value (n = 213)	1.00		1.00	
>40% value (n = 320)	1.16 (0.85-1.59)	0.34	1.17 (0.85-1.61)	0.34
ETS1 (cut-off 12.51)				
≤40% value (n = 213)	1.00		1.00	
>40% value (n = 320)	0.59 (0.44-0.80)	0.001	0.58 (0.43-0.78)	<0.001

CI, confidence interval; RCC, renal cell carcinoma.

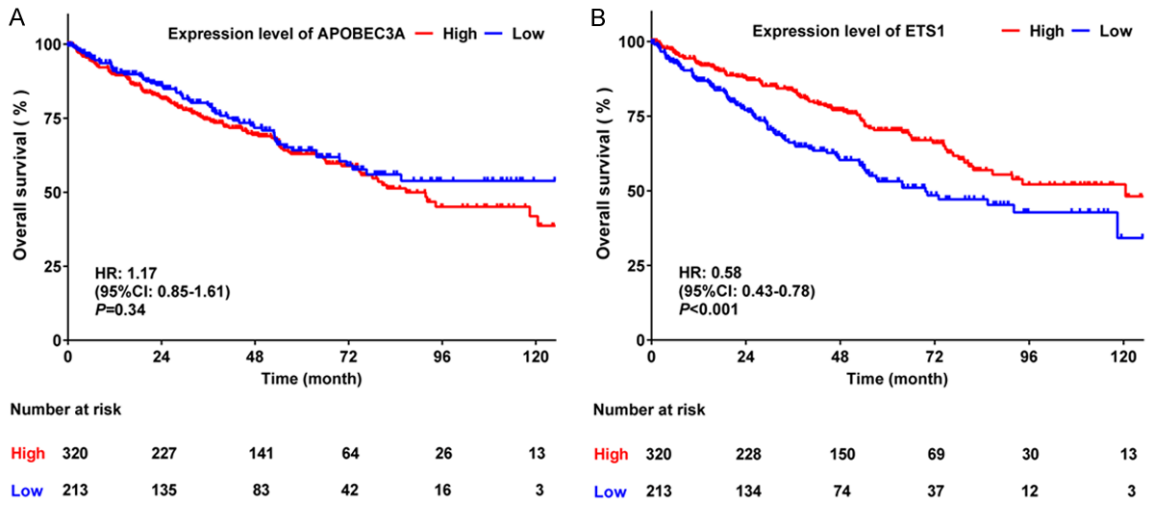

Figure 5. Prognostic value of A3A and ETS1 expression in tumors on overall survival of ccRCC patients by Kaplan-Meier analysis. A. No significance was detected between the expression of A3A and the prognosis of ccRCC patients. B. High expression of ETS1 was significantly related to a favorable prognosis in ccRCC.

drug in bladder cancer cell lines [20, 37]. A3A expression was up-regulated as part of the antiviral interferon-stimulated response in breast cancer cell lines [37]. In this study, we found that the promoter activity of *A3A* was up-regulated in most of cell lines (786-O, A498, ACHN, SW620) by PMA and all the RCC and colorectal cancer cells by TNFα, rather than by IL-6 stimulation. Furthermore, the activity of the *A3A* promoter carrying rs12157810-C, rather than that carrying rs12157810-A, was specifically up-regulated via TNF-α stimulation in RCC cells. PMA is a powerful tumor promoter and activator of protein kinase C, a kinase that is present in transitional points of many cell signaling pathways including NF-κB [38]. TNFα is the prominent activator of NF-κB signaling pathway [39]. Thus, the activity of the A3A promoter carrying rs12157810-C in RCC cells is specifically up-regulated via TNFα/NF-κB, rather than IL-6/STAT3 inflammatory signaling pathway.

ETS1 is generally considered as an oncogenic factor because of aberrant overexpression in human cancer, pro-angiogenesis, and involve-

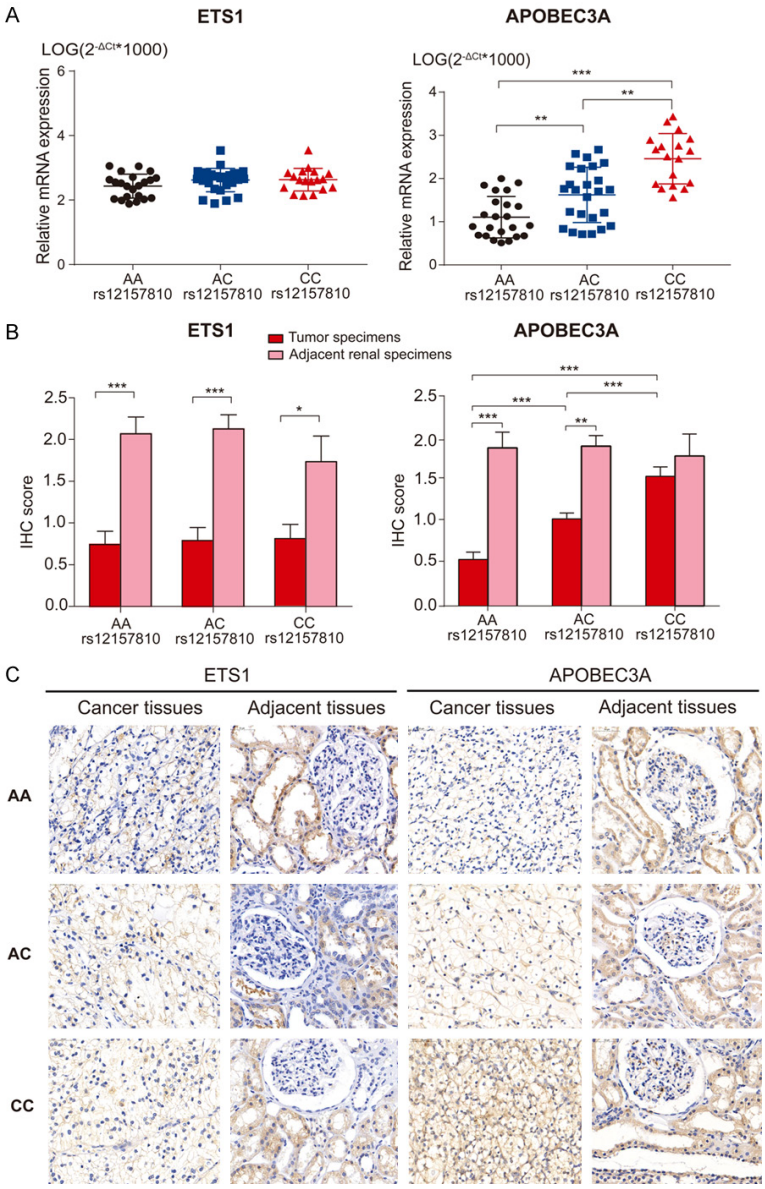

Figure 6. Association of the genotype at rs12157810 with the expression of A3A/ETS1. A. The levels of *ETS1* and *A3A* transcriptions in the surgically removed FFPE specimens of ccRCC patients with different genotypes at rs12157810. B. The difference in the expression of *A3A* and *ETS1* protein between the ccRCC and matched adjacent tissues of ccRCC patients with different genotypes at rs12157810. C. Representative immunohistochemistry staining of ETS1 and A3A expression in ccRCC and adjacent tissues of patients with different genotypes at rs12157810. $^{*}P<0.05$, $^{**}P<0.01$, $^{***}P<0.001$.

ment in MAPK signaling pathway [33]. It is also involved in the transcription of telomerase reverse transcriptase (TERT) via reactivating the mutant TERT promoter, thus promoting the development of cancers [40, 41]. However, ETS1 was also found to bind to wild-type p53 preferentially, raising its tumor-suppressive role [42]. The role of ETS1 in RCC remains unknown. In this study, we identified that *ETS1* was a prominent transcriptional repressor of the *A3A* promoter. The repressive effect of *ETS1* to the sequence with rs12157810-A was predicted to be higher than that with rs12157810-C (**Table 2**). Our multivariate Cox regression analysis also found that ETS1 expression in tumors independently predicted a favorable prognosis in ccRCC (**Table 3**; **Figure 5**). The levels of ETS1 in the tumor tissues were significantly lower than that in the adjacent tissues of each genotype ($P<0.05$, **Figure 6B**, **6C**). These evidences convincingly indicate that *ETS1* functions as a tumor suppressor in ccRCC.

Our ChIP-qPCR experiments demonstrated that the physical binding effects of ETS1 to the genomic DNAs of 786-O, a ccRCC cell line with rs12157810-AC, and A498 and Caki2, the ccRCC cell lines with rs12157810-CC, were more specific than that of ACHN, a papillary RCC cell line with rs12157810-AA (**Figure 4D**). These data indicate that ETS1 can bind more the A3A promoter with rs12157810-C than the promoter with rs12157810-A. That is, the A3A promoter with rs12157810-C binds less ETS1 than does the A3A promoter with rs12157810-A. Furthermore, siETS1 greatly up-regulated the activity of the A3A promoter with rs12157810-C in four of six cell lines and down-regulated the activity of the A3A promoter with rs12157810-A in two of the six cell lines (**Figure 4F**), indicating potential co-repressors that bind the *A3A* promoter with A or C at rs12157810 do exist. Knockdown of RFX5 and ZEB1 significantly increased

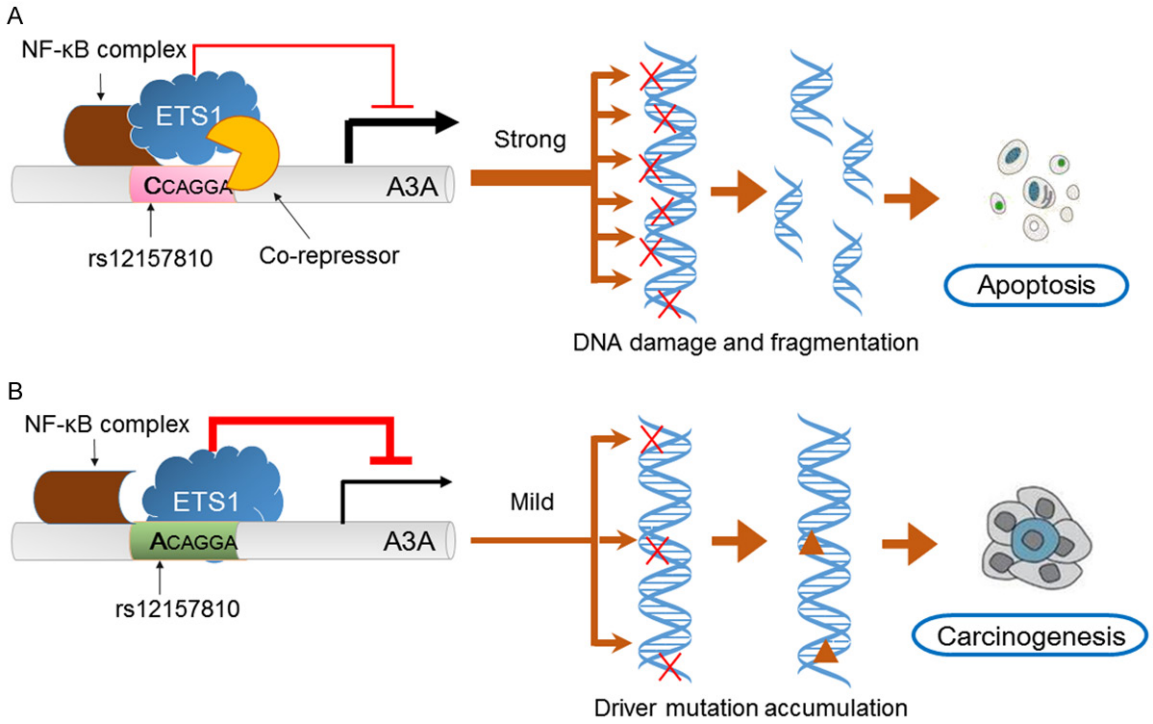

Figure 7. The possible mechanism of regulating A3A expression and consequences. A. Strong mode: ETS1 loosely binds to the *A3A* promoter with rs12157810-C together with some co-repressors such as RFX5 and ZEB1 and predominantly controls the transcription of *A3A*. NF-κB complex *trans*-activates the *A3A* promoter with rs12157810-C more potently than does the promoter with rs12157810-A. Higher A3A expression results in more fragmentation of the genome, resulting in cell apoptosis. B. Mild mode: ETS1 tensely binds to the *A3A* promoter with rs12157810-A. Under the control of NF-κB complex and ETS1, *A3A* mildly and consistently expresses and exhibits a relatively low level of mutagenic function, thus accumulating the driver mutations that initiate carcinogenesis.

the expression of A3A in 786-O cells, rather than in ACHN (**Figure 4B**), indicating that RFX5 and ZEB1 might be co-repressors for the A3A promoter with rs12157810-C.

Figure 7 is depicted to better illustrate the possible mechanism of regulating A3A expression and consequences. Two modes of A3A regulation by ETS1 are proposed: A, strong mode; B, mild mode. In A mode that is specific for population with rs12157810-C allele, ETS1 loosely binds to the *A3A* promoter with rs12157810-C together with some co-repressors such as RFX5 and ZEB1 and predominantly controls the transcription of *A3A*. The *A3A* promoter with rs12157810-C increases the transcription of *A3A* more potently than does the promoter with rs12157810-A. Higher expression of A3A leads to more fragmentation of the genome, resulting in cell apoptosis. In B mode that is specific for population with rs12157810-A allele, ETS1 tensely binds to the *A3A* promoter with rs12157810-A. *A3A* mildly and consistently expresses and exhibits a relatively low level of mutagenic function, thus accumulating the driver mutations that initiate carcinogenesis.

Our study had limitations. First, the potent co-repressors that repressed the activity of the *A3A* promoter with rs12157810-C need to be further identified. Second, the effect of reciprocal inhibition or mutual regulation between ETS1 and NF-κB signaling factor(s) on A3A expression was not investigated. Third, the enrolled 728 RCC patients were not included in the prognosis analysis because the follow-up duration was too short to obtain a sufficient number of patients with the end-point event.

In summary, the present study revealed that the *A3A* promoter with rs12157810-C, a polymorphic allele that facilitated the expression of A3A, was significantly associated with a decreased risk of RCC. The increased level of A3A expression increases the apoptosis of

RCC cells, possibly because higher mutagenic activity greatly increases genomic DNA fragmentation. Furthermore, the activity of the *A3A* promoter with rs12157810-C in RCC cells was proven to be transcriptionally activated by TNF-α/NF-κB signaling pathway and predominantly repressed by ETS1. High-level ETS1 expression in tumors predicts a favorable prognosis in ccRCC independently. ETS1 might function as a tumor suppressor in ccRCC. These findings are novel and may provide important clues to elucidate the mechanisms by which the imbalance of APOBEC-UNG influences the development of ccRCC. The outcomes of this study may be predictive and prognostic for ccRCC.

Acknowledgements

This work was supported by the National Natural Science Foundation of China (81520108021, 81672518, 81903388).

Disclosure of conflict of interest

None.

Address correspondence to: Guangwen Cao, Department of Epidemiology, Second Military Medical University, Shanghai 200433, China. Tel: +86-21-81871060; Fax: +86-21-81871060; E-mail: gcao@smmu.edu.cn

References

[1] Bray F, Ferlay J, Soerjomataram I, Siegel RL, Torre LA and Jemal A. Global cancer statistics 2018: GLOBOCAN estimates of incidence and mortality worldwide for 36 cancers in 185 countries. CA Cancer J Clin 2018; 68: 394-424.

[2] Znaor A, Lortet-Tieulent J, Laversanne M, Jemal A and Bray F. International variations and trends in renal cell carcinoma incidence and mortality. Eur Urol 2015; 67: 519-530.

[3] Chow WH, Dong LM and Devesa SS. Epidemiology and risk factors for kidney cancer. Nat Rev Urol 2010; 7: 245-257.

[4] Wang G, Hou J, Ma L, Xie J, Yin J, Xu D, Chang W, Tan X, Su T, Zhang H and Cao G. Risk factor for clear cell renal cell carcinoma in Chinese population: a case-control study. Cancer Epidemiol 2012; 36: 177-182.

[5] Melkonian SC, Daniel CR, Ye Y, Tannir NM, Karam JA, Matin SF, Wood CG and Wu X. Gene-environment interaction of genome-wide association study-identified susceptibility loci and meat-cooking mutagens in the etiology of renal cell carcinoma. Cancer 2016; 122: 108-115.

[6] Swanton C, McGranahan N, Starrett GJ and Harris RS. APOBEC enzymes: mutagenic fuel for cancer evolution and heterogeneity. Cancer Discov 2015; 5: 704-12.

[7] Seplyarskiy VB, Andrianova MA and Bazykin GA. APOBEC3A/B-induced mutagenesis is responsible for 20% of heritable mutations in the TpCpW context. Genome Res 2017; 27: 175-184.

[8] Suspène R, Aynaud MM, Guétard D, Henry M, Eckhoff G, Marchio A, Pineau P, Dejean A, Vartanian JP and Wain-Hobson S. Somatic hypermutation of human mitochondrial and nuclear DNA by APOBEC3 cytidine deaminases, a pathway for DNA catabolism. Proc Natl Acad Sci U S A 2011; 108: 4858-4863.

[9] Nik-Zainal S, Wedge DC, Alexandrov LB, Petljak M, Butler AP, Bolli N, Davies HR, Knappskog S, Martin S, Papaemmanuil E, Ramakrishna M, Shlien A, Simonic I, Xue Y, Tyler-Smith C, Campbell PJ and Stratton MR. Association of a germline copy number polymorphism of APOBEC3A and APOBEC3B with burden of putative APOBEC-dependent mutations in breast cancer. Nat Genet 2014; 46: 487-91.

[10] Wang XM, Lu Y, Song YM, Dong J, Li RY, Wang GL, Wang X, Zhang SD, Dong ZH, Lu M, Wang SY, Ge LY, Luo GD, Ma RZ, George Rozen S, Bai F, Wu D and Ma LL. Integrative genomic study of Chinese clear cell renal cell carcinoma reveals features associated with thrombus. Nat Commun 2020; 11: 739.

[11] Green AM, Budagyan K, Hayer KE, Reed MA, Savani MR, Wertheim GB and Weitzman MD. Cytosine deaminase APOBEC3A sensitizes leukemia cells to inhibition of the DNA replication checkpoint. Cancer Res 2017; 77: 4579-4588.

[12] Green AM, Landry S, Budagyan K, Avgousti DC, Shalhout S, Bhagwat AS and Weitzman MD. APOBEC3A damages the cellular genome during DNA replication. Cell Cycle 2016; 15: 998-1008.

[13] Liu WB and Cao GW. The role of APOBEC3B in the development of hepatocellular carcinoma should be investigated with the consideration of hepatitis B virus evolution. Hepatoma Res 2019; 5: 30.

[14] Burns MB, Temiz NA and Harris RS. Evidence for APOBEC3B mutagenesis in multiple human cancers. Nat Genet 2013; 45: 977-983.

[15] Petljak M, Alexandrov LB, Brammeld JS, Price S, Wedge DC, Grossmann S, Dawson KJ, Ju YS, Iorio F, Tubio JMC, Koh CC, Georgakopoulos-Soares I, Rodríguez-Martín B, Otlu B, O'Meara S, Butler AP, Menzies A, Bhosle SG, Raine K, Jones DR, Teague JW, Beal K, Latimer C, O'Neill L, Zamora J, Anderson E, Patel N, Maddison M,

Ng BL, Graham J, Garnett MJ, McDermott U, Nik-Zainal S, Campbell PJ and Stratton MR. Characterizing mutational signatures in human cancer cell lines reveals episodic APOBEC mutagenesis. Cell 2019; 176: 1282-1294, e20.

[16] Walker BA, Wardell CP, Murison A, Boyle EM, Begum DB, Dahir NM, Proszek PZ, Melchor L, Pawlyn C, Kaiser MF, Johnson DC, Qiang YW, Jones JR, Cairns DA, Gregory WM, Owen RG, Cook G, Drayson MT, Jackson GH, Davies FE and Morgan GJ. APOBEC family mutational signatures are associated with poor prognosis translocations in multiple myeloma. Nat Commun 2015; 6: 6997.

[17] Nakamura H, Arai Y, Totoki Y, Shirota T, Elzawahry A, Kato M, Hama N, Hosoda F, Urushidate T, Ohashi S, Hiraoka N, Ojima H, Shimada K, Okusaka T, Kosuge T, Miyagawa S and Shibata T. Genomic spectra of biliary tract cancer. Nat Genet 2015; 47: 1003-1010.

[18] Chen TW, Lee CC, Liu H, Wu CS, Pickering CR, Huang PJ, Wang J, Chang IY, Yeh YM, Chen CD, Li HP, Luo JD, Tan BC, Chan TEH, Hsueh C, Chu LJ, Chen YT, Zhang B, Yang CY, Wu CC, Hsu CW, See LC, Tang P, Yu JS, Liao WC, Chiang WF, Rodriguez H, Myers JN, Chang KP and Chang YS. APOBEC3A is an oral cancer prognostic biomarker in Taiwanese carriers of an APOBEC deletion polymorphism. Nat Commun 2017; 8: 465.

[19] Serebrenik AA, Starrett GJ, Leenen S, Jarvis MC, Shaban NM, Salamango DJ, Nilsen H, Brown WL and Harris RS. The deaminase APOBEC3B triggers the death of cells lacking uracil DNA glycosylase. Proc Natl Acad Sci U S A 2019; 116: 22158-22163.

[20] Liu W, Wu J, Yang F, Ma L, Ni C, Hou X, Wang L, Xu A, Song J, Deng Y, Xian L, Li Z, Wang S, Chen X, Yin J, Han X, Li C, Zhao J and Cao G. Genetic polymorphisms predisposing the interleukin 6-induced APOBEC3B-UNG imbalance increase HCC risk via promoting the generation of APOBEC-signature HBV mutations. Clin Cancer Res 2019; 25: 5525-5536.

[21] Deng Y, Du Yang, Zhang Qi, Han X and Cao GW. Human cytidine deaminases facilitate hepatitis B virus evolution and link inflammation and hepatocellular carcinoma. Cancer Lett 2014; 343: 161-171.

[22] Knisbacher BA, Gerber D and Levanon EY. DNA editing by APOBECs: a genomic preserver and transformer. Trends Genet 2016; 32: 16-28.

[23] Tan X, He S, Han Y, Yu Y, Xiao J, Xu D, Wang G, Du Y, Chang W, Yin J, Su T, Hou J and Cao G. Establishment and characterization of clear cell renal cell carcinoma cell lines with different metastatic potential from Chinese patients. Cancer Cell Int 2013; 13: 20.

[24] Camp RL, Dolled-Filhart M and Rimm DL. X-tile: a new bio-informatics tool for biomarker assessment and outcome-based cut-point optimization. Clin Cancer Res 2004; 10: 7252-7259.

[25] Liu Y, Han X, Yu Y, Ding Y, Ni C, Liu W, Hou X, Li Z, Hou J, Shen D, Yin J, Zhang H, Thompson TC, Tan X and Cao G. A genetic polymorphism affects the risk and prognosis of renal cell carcinoma: association with follistatin-like protein 1 expression. Sci Rep 2016; 6: 26689.

[26] Gudbrandsdottir G, Aarstad HH, Bostad L, Hjelle KM, Aarstad HJ, Bruserud Ø, Tvedt THA and Beisland C. Serum levels of the IL-6 family of cytokines predict prognosis in renal cell carcinoma (RCC). Cancer Immunol Immunother 2021; 70: 19-30.

[27] Quan Z, He Y, Luo C, Xia Y, Zhao Y, Liu N and Wu X. Interleukin 6 induces cell proliferation of clear cell renal cell carcinoma by suppressing hepaCAM via the STAT3-dependent up-regulation of DNMT1 or DNMT3b. Cell Signal 2017; 32: 48-58.

[28] Wang Y, Su J, Wang Y, Fu D, Ideozu JE, Geng H, Cui Q, Wang C, Chen R, Yu Y, Niu Y and Yue D. The interaction of YBX1 with G3BP1 promotes renal cell carcinoma cell metastasis via YBX1/G3BP1-SPP1-NF-κB signaling axis. J Exp Clin Cancer Res 2019; 38: 386.

[29] Qi H and Ohh M. The von Hippel-Lindau tumor suppressor protein sensitizes renal cell carcinoma cells to tumor necrosis factor-induced cytotoxicity by suppressing the nuclear factor-kappaB-dependent antiapoptotic pathway. Cancer Res 2003; 63: 7076-7080.

[30] Green AM, Budagyan K, Hayer KE, Reed MA, Savani MR, Wertheim GB and Weitzman MD. Cytosine deaminase APOBEC3A sensitizes leukemia cells to inhibition of the DNA replication checkpoint. Cancer Res 2017; 77: 4579-4588.

[31] Li X, Caval V, Wain-Hobson S and Vartanian JP. Elephant APOBEC3A cytidine deaminase induces massive double-stranded DNA breaks and apoptosis. Sci Rep 2019; 9: 728.

[32] Madison BJ, Clark KA, Bhachech N, Hollenhorst PC, Graves BJ and Currie SL. Electrostatic repulsion causes anticooperative DNA binding between tumor suppressor ETS transcription factors and JUN-FOS at composite DNA sites. J Biol Chem 2018; 293: 18624-18635.

[33] Teng Y, Cang B, Mao F, Chen W, Cheng P, Peng L, Luo P, Lu D, You N, Zou Q and Zhuang Y. Expression of ETS1 in gastric epithelial cells positively regulate inflammatory response in Helicobacter pylori-associated gastritis. Cell Death Dis 2020; 11: 498.

[34] Dittmer J. The role of the transcription factor Ets1 in carcinoma. Semin Cancer Biol 2015; 35: 20-38.

[35] Jalili P, Bowen D, Langenbucher A, Park S, Aguirre K, Corcoran RB, Fleischman AG, Lawrence MS, Zou L and Buisson R. Quantification of on-

going APOBEC3A activity in tumor cells by monitoring RNA editing at hotspots. Nat Commun 2020; 11: 2971.

[36] Cortez LM, Brown AL, Dennis MA, Collins CD, Brown AJ, Mitchell D, Mertz TM and Roberts SA. APOBEC3A is a prominent cytidine deaminase in breast cancer. PLoS Genet 2019; 15: e1008545.

[37] Middlebrooks CD, Banday AR, Matsuda K, Udquim KI, Onabajo OO, Paquin A, Figueroa JD, Zhu B, Koutros S, Kubo M, Shuin T, Freedman ND, Kogevinas M, Malats N, Chanock SJ, Garcia-Closas M, Silverman DT, Rothman N and Prokunina-Olsson L. Association of germline variants in the APOBEC3 region with cancer risk and enrichment with APOBEC-signature mutations in tumors. Nat Genet 2016; 48: 1330-1338.

[38] Babu RL, Naveen Kumar M, Patil RH, Kiran Kumar KM, Devaraju KS, Ramesh GT and Sharma SC. Forskolin and Phorbol 12-myristate 13-acetate modulates the expression pattern of AP-1 factors and cell cycle regulators in estrogen-responsive MCF-7 cells. Genes Dis 2018; 6: 159-166.

[39] Aggarwal BB, Vijayalekshmi RV and Sung B. Targeting inflammatory pathways for prevention and therapy of cancer: short-term friend, long-term foe. Clin Cancer Res 2009; 15: 425-430.

[40] Xu X, Li Y, Bharath SR, Ozturk MB, Bowler MW, Loo BZL, Tergaonkar V and Song H. Structural basis for reactivating the mutant TERT promoter by cooperative binding of p52 and ETS1. Nat Commun 2018; 9: 3183.

[41] Ma ZX, Yang CM, Li MG and Tu H. Telomerase reverse transcriptase promoter mutations in hepatocellular carcinogenesis. Hepatoma Res 2019; 5: 8.

[42] Suzuki H, Romano-Spica V, Papas TS and Bhat NK. ETS1 suppresses tumorigenicity of human colon cancer cells. Proc Natl Acad Sci U S A 1995; 92: 4442-4446.

Table S1. Sequences of primers, probes, and siRNAs

SNP or Gene	Primers and Probes	Sequence (5'-3')
Primers and probes for SNP genotyping		
rs12157810	Forward Primer	CAGCCAGGGAAGAAGATGCA
	Reverse Primer	CCTGGAGAAAGACCCTGAATAACA
	Probe 1	FAM-CCTAACAGAGAGCCCAG-MGB
	Probe 2	HEX-CAGAGAGCACAGGAT-MGB
rs12628403	Forward Primer	AACTGCCTGATGAAGGAGCTAAGT
	Reverse Primer	GATAAGTCACGCTCCCGCTG
	Probe 1	FAM-CTGAGAGTCATGGGC-MGB
	Probe 2	HEX-CTGAGAGTCCTGGGC-MGB
rs2267401	Forward Primer	CTCAAAGCTCTGGGCACACA
	Reverse Primer	ACGGAATTGCAAAGAGAAAGAGA
	Probe 1	FAM-CTCCCAGGCGCAGG-MGB
	Probe 2	HEX-CCCAGGCTCAGGCT-MGB
rs1174657	Forward Primer	CCACTATCTCCACTGACCTTCC
	Reverse Primer	CCCAGGAATATCGTAAGGCA
	Probe 1	FAM-AGGTCCTCGGTTTC-MGB
	Probe 2	VIC-AAGGTCCTTGGTTTC-MGB
rs3890995	Forward Primer	TCCTCCTGCCCCACTTTCTA
	Reverse Primer	GACAGAAACACACAAGGAAAGAATAAA
	Probe 1	FAM-CATTGCTCTTTAACTGCTA-MGB
	Probe 2	TET-CCATTGCTCTCTAACT-MGB
Primers for quantification RT-PCR		
GAPDH	Forward Primer	CTGGACCGTCTCAAGGTGTT
	Reverse Primer	GCCCCAGATAGGCAAACTT
APOBEC3A	Forward Primer	GACACTTGATGGATCCACAC
	Reverse Primer	AAGATTCTTAGCCTGGTTGTG
ETS1	Forward Primer	GATAGTTGTGATCGCCTCACC
	Reverse Primer	GTCCTCTGAGTCGAAGCTGTC
Primers for ChIP-qPCR		
APOBEC3A promoter	Forward Primer	CCTGCTGGTCTC CCATCTT
	Reverse Primer	AGAGCAGGCTCCAGGACA
siRNAs for gene knock down		
ETS1	siETS1	GGAATTACTCACTGATAAA
RFX5	siRFX5	GCAAGATCATCAGAGAGAT
ZEB1	siZEB1	GGCCTGAAATCCTCTCGAA
MSX2	siMSX2	GGCAGC GTCCATATATGGA

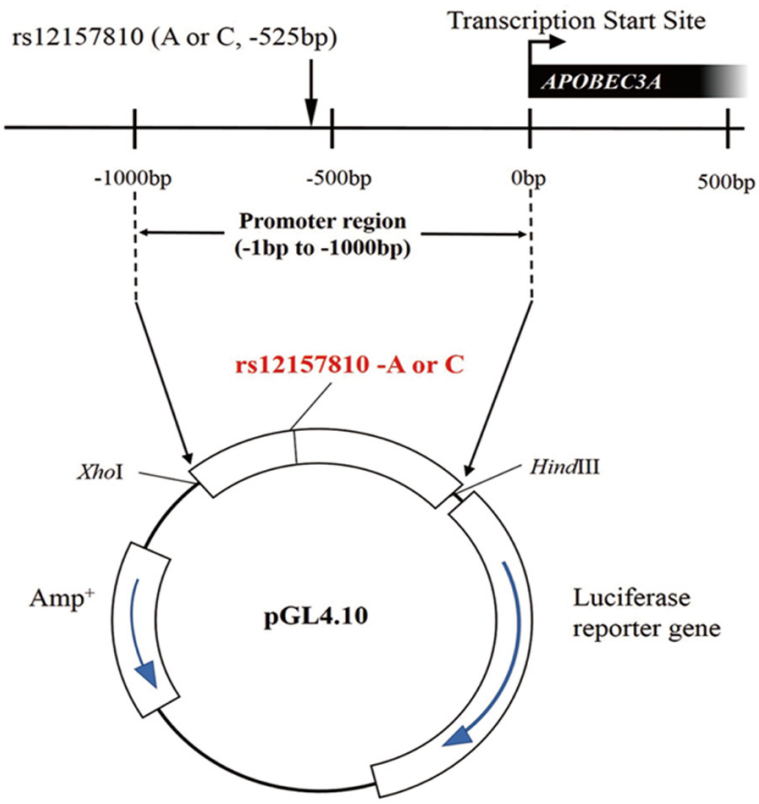

Figure S1. The schematic structure of reporter vectors whose luciferase reporter gene is under the transcriptional control of the A3A promoter with different alleles at rs12157810.

Table S2. Associations of *APOBEC/UNG* polymorphisms with the risk of RCC in each gender

SNP	SNP genotype	RCC patients (%)		Health control (%)		RCC versus control AOR (95% CI)	
		Male	Female	Male	Female	Male	Female
rs12157810 (*APOBEC3A* -525 bp A>C)	AA	304 (60.08)	127 (59.62)	581 (55.70)	210 (53.57)	1.00	1.00
	AC	168 (33.20)	73 (34.72)	309 (29.63)	126 (32.14)	1.04 (0.82-1.31)	0.97 (0.68-1.40)
	CC	34 (6.72)	13 (6.10)	153 (14.67)	56 (14.29)	0.42 (0.28-0.62)	0.40 (0.21-0.77)
	AC+CC	202 (39.92)	86 (40.38)	462 (44.30)	182 (46.43)	0.86 (0.70-1.07)	0.91 (0.65-1.27)
rs12628403 (*APOBEC3A* 4340 bp A>C)	AA	210 (41.42)	98 (47.12)	445 (41.94)	172 (41.05)	1.00	1.00
	AC	235 (46.35)	71 (34.13)	496 (46.75)	206 (49.16)	1.01 (0.80-1.26)	0.60 (0.42-0.86)
	CC	62 (12.23)	39 (18.75)	120 (11.31)	41 (9.79)	1.10 (0.76-1.55)	1.61 (0.97-2.67)
	AC+CC	297 (58.58)	110 (52.88)	616 (58.06)	247 (58.95)	1.04 (0.84-1.28)	0.77 (0.55-1.07)
rs2267401* (*APOBEC3B* -338 bp T>G)	TT	95 (45.24)	28 (28.87)	166 (38.52)	63 (37.28)	1.00	1.00
	TG	79 (37.62)	47 (48.45)	196 (45.48)	71 (42.01)	0.71 (0.49-1.14)	1.47 (0.82-2.62)
	GG	36 (17.14)	22 (22.68)	69 (16.01)	35 (20.71)	0.91 (0.57-1.47)	1.30 (0.70-2.80)
	TG+GG	115 (54.76)	69 (71.13)	265 (61.48)	106 (62.72)	0.76 (0.54-1.06)	0.76 (0.54-1.06)
rs1174657 (*APOBEC4* 5526 bp T>C)	TT	315 (61.75)	141 (65.58)	636 (64.70)	256 (65.31)	1.00	1.00
	TC	178 (34.90)	65 (30.23)	295 (30.01)	116 (29.59)	1.22 (0.97-1.52)	1.03 (0.71-1.49)
	CC	17 (3.33)	9 (4.19)	52 (5.29)	20 (5.10)	0.66 (0.38-1.16)	0.88 (0.39-2.00)
	TC+CC	195 (38.24)	74 (34.42)	347 (35.30)	136 (34.69)	1.15 (0.92-1.44)	1.03 (0.73-1.47)
rs3890995 (*UNG* -1956 bp T>C)	TT	202 (40.89)	87 (41.63)	453 (43.23)	181 (43.30)	1.00	1.00
	TC	232 (46.96)	89 (42.58)	475 (45.32)	179 (42.82)	1.09 (0.87-1.37)	1.05 (0.73-1.51)
	CC	60 (12.15)	33 (15.79)	120 (11.45)	58 (13.88)	1.12 (0.79-1.60)	1.16 (0.70-1.91)
	TC+CC	292 (59.11)	122 (58.37)	595 (56.77)	237 (56.70)	1.10 (0.88-1.37)	1.07 (0.77-1.51)

SNP, single-nucleotide polymorphism; HCC, hepatocellular carcinoma; HBV, hepatitis B virus; CI, confidence interval. AOR, Odds ratio adjusted for age. *Calculated in subjects with rs12628403-AA genotype (without APOBEC3B-deletion).

Table S3. Associations of *APOBEC3* and *UNG* polymorphisms with the risk of different subtypes of RCC

Variable		Papillary carcinomas, n (%)	Chromophobe carcinomas, n (%)	Other subtypes, n (%)	Healthy control, n (%)	AOR for Papillary carcinomas (95% CI)	AOR for Chromophobe carcinomas (95% CI)	AOR for Other subtypes of RCC (95% CI)
Age (year)		57.85±2.70	50.43±1.97	55.25±2.51	56.03±0.39	1.008 (0.98-1.03)	0.97 (0.94-1.003)	0.99 (0.97-1.02)
Gender								
Female		7 (20.59)	12 (52.17)	6 (25.00)	425 (28.33)	1.00	1.00	1.00
Male		27 (79.41)	11 (47.83)	18 (75.00)	1075 (71.67)	1.52 (0.65-3.52)	0.36 (0.15-0.82)	1.18 (0.46-3.008)
rs12157810 (*APOBEC3A* -525 bp A>C)	AA	19 (55.88)	12 (57.14)	12 (50.0)	791 (55.12)	1.00	1.00	1.00
	AC	12 (35.29)	9 (42.86)	9 (37.5.0)	435 (30.31)	1.14 (0.53-2.36)	1.30 (0.52-3.12)	1.37 (0.55-3.27)
	CC	3 (8.82)	0 (0)	3 (12.5.0)	209 (14.57)	0.58 (0.13-1.76)	-	0.93 (0.21-3.02)
	AC+CC	15 (44.12)	9 (42.86)	12 (50.00)	644 (44.88)	0.98 (0.48-1.94)	0.85 (0.34-2.04)	1.22 (0.53-2.77)
	A allele	50 (73.53)	33 (78.57)	33 (68.75)	2017 (70.28)	1.00	1.00	1.00
	C allele	18 (26.47)	9 (21.43)	15 (31.25)	853 (29.72)	0.86 (0.48-1.46)	0.59 (0.26-1.19)	1.06 (0.55-1.93)
rs12628403 (*APOBEC3A* 4340 bp A>C)	AA	14 (42.42)	15 (65.22)	12 (50.00)	617 (41.69)	1.00	1.00	1.00
	AC	16 (48.48)	5 (21.74)	8 (33.33)	702 (47.43)	0.99 (0.48-2.08)	0.29 (0.09-0.76)	0.58 (0.23-1.42)
	CC	3 (9.09)	3 (13.04)	4 (16.67)	161 (10.88)	0.84 (0.19-2.64)	0.83 (0.19-2.61)	1.28 (0.35-3.75)
	AC+CC	19 (57.58)	8 (34.78)	12 (50.00)	863 (58.31)	0.96 (0.48-1.97)	0.38 (0.15-0.89)	0.71 (0.32-1.63)
	A allele	44 (66.67)	35 (76.09)	32 (66.67)	1936 (65.41)	1.00	1.00	1.00
	C allele	22 (33.33)	11 (23.91)	16 (33.33)	1024 (34.59)	0.94 (0.55-1.56)	0.61 (0.29-1.17)	0.95 (0.51-1.71)
rs2267401* (*APOBEC3B* -338 bp T>G)	TT	7 (53.85)	7 (53.85)	8 (53.33)	229 (38.17)	1.00	1.00	1.00
	TG	4 (30.77)	4 (30.77)	5 (33.33)	267 (44.50)	0.48 (0.12-1.64)	0.54 (0.16-1.67)	0.42 (0.08-1.64)
	GG	2 (15.38)	2 (15.38)	2 (13.33)	104 (17.33)	0.63 (0.09-2.70)	0.56 (0.08-2.30)	1.12 (0.23-4.33)
	TG+GG	6 (46.15)	6 (46.15)	7 (46.67)	371 (61.83)	0.52 (0.16-1.58)	0.53 (0.18-1.52)	0.61 (0.19-1.99)
	T allele	18 (69.23)	21 (70)	15 (62.5)	725 (60.42)	1.00	1.00	1.00
	G allele	8 (30.77)	9 (30)	9 (37.5)	475 (39.58)	0.66 (0.26-1.49)	0.64 (0.27-1.37)	0.91 (0.38-2.07)
rs1174657 (*APOBEC4* 5526 bp T>C)	TT	22 (64.71)	18 (78.26)	13 (54.17)	892 (64.87)	1.00	1.00	1.00
	TC	9 (26.47)	5 (21.74)	10 (41.67)	411 (29.89)	0.88 (0.38-1.89)	0.60 (0.19-1.53)	1.67 (0.71-3.82)
	CC	3 (8.82)	0 (0)	1 (4.17)	72 (5.24)	1.70 (0.39-5.06)	-	0.94 (0.05-4.84)
	TC+CC	12 (35.29)	5 (21.74)	11 (45.83)	483 (35.13)	1.01 (0.47-2.03)	0.51 (0.16-1.29)	1.56 (0.68-3.51)
	T allele	1025 (79.58)	53 (80.3)	41 (89.13)	2195 (79.82)	1.00	1.00	1.00
	C allele	263 (20.42)	13 (19.7)	5 (10.87)	555 (20.18)	1.02 (0.86-1.19)	1.12 (0.60-1.96)	0.47 (0.16-1.11)
rs3890995 (*UNG* -1956 bp T>C)	TT	14 (42.42)	4 (18.18)	8 (34.78)	634 (43.22)	1.00	1.00	1.00
	TC	12 (36.36)	15 (68.18)	12 (52.17)	655 (44.65)	0.83 (0.37-1.81)	3.62 (1.30-12.78)	1.45 (0.59-3.71)
	CC	7 (21.21)	3 (13.64)	3 (13.04)	178 (12.13)	1.81 (0.67-4.44)	2.61 (0.51-11.98)	1.35 (0.29-4.74)
	TC+CC	19 (57.58)	18 (81.82)	15 (65.22)	833 (56.78)	1.04 (0.52-2.13)	3.41 (1.26-11.86)	1.42 (0.61-3.55)
	T allele	40 (60.61)	23 (52.27)	28 (60.87)	1923 (65.54)	1.00	1.00	1.00
	C allele	26 (39.39)	21 (47.73)	18 (39.13)	1011 (34.46)	1.24 (0.74-2.03)	1.72 (0.94-3.14)	1.22 (0.66-2.21)

SNP, single-nucleotide polymorphism; CI, confidence interval. AOR, Odds ratio adjusted for age and gender. *Calculated in subjects with rs12628403-AA genotype (without APOBEC3B-deletion).

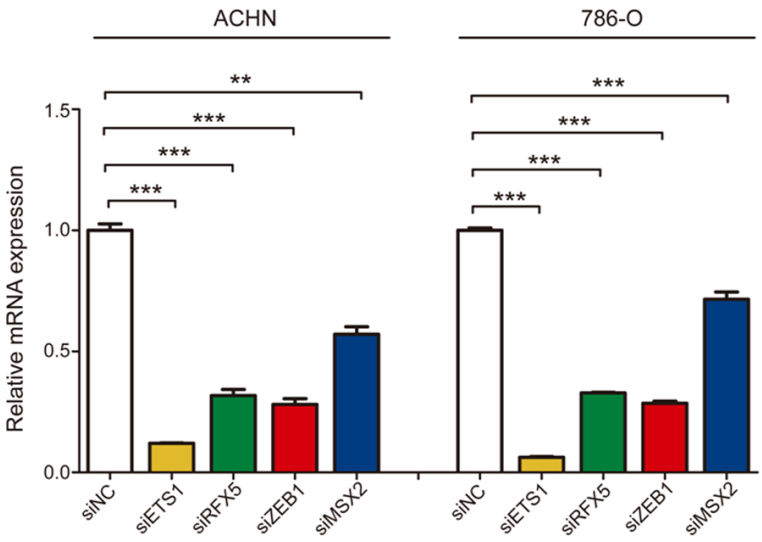

Figure S2. The knockdown effects of siRNA targeting the candidate transcriptional repressors on the expression of A3A as detected by quantitative RT-PCR.